Pharmaceutical Research, Vol. 26, No. 7, July 2009 (© 2009)
DOI: 10.1007/s11095-009-9868-4

Research Paper

Phase Transitions in Frozen Systems and During Freeze–Drying: Quantification Using Synchrotron X-Ray Diffractometry

Dushyant B. Varshney,[1,2,5] Prakash Sundaramurthi,[1] Satyendra Kumar,[3] Evgenyi Y. Shalaev,[4] Shin-Woong Kang,[3] Larry A. Gatlin,[4] and Raj Suryanarayanan[1,5]

Received December 23, 2008; accepted February 26, 2009; published online March 27, 2009

Purpose. (1) To develop a synchrotron X-ray diffraction (SXRD) method to monitor phase transitions during the entire freeze–drying cycle. Aqueous sodium phosphate buffered glycine solutions with initial glycine to buffer molar ratios of 1:3 (17:50 mM), 1:1 (50 mM) and 3:1 were utilized as model systems. (2) To investigate the effect of initial solute concentration on the crystallization of glycine and phosphate buffer salt during lyophilization.

Methods. Phosphate buffered glycine solutions were placed in a custom-designed sample cell for freeze–drying. The sample cell, covered with a stainless steel dome with a beryllium window, was placed on a stage capable of controlled cooling and vacuum drying. The samples were cooled to −50°C and annealed at −20°C. They underwent primary drying at −25°C under vacuum until ice sublimation was complete and secondary drying from 0 to 25°C. At different stages of the freeze–drying cycle, the samples were periodically exposed to synchrotron X-ray radiation. An image plate detector was used to obtain time-resolved two-dimensional SXRD patterns. The ice, β-glycine and DHPD phases were identified based on their unique X-ray peaks.

Results. When the solutions were cooled and annealed, ice formation was followed by crystallization of disodium hydrogen phosphate dodecahydrate (DHPD). In the primary drying stage, a significant increase in DHPD crystallization followed by incomplete dehydration to amorphous disodium hydrogen phosphate was evident. Complete dehydration of DHPD occurred during secondary drying. Glycine crystallization was inhibited throughout freeze–drying when the initial buffer concentration (1:3 glycine to buffer) was higher than that of glycine.

Conclusion. A high-intensity X-ray diffraction method was developed to monitor the phase transitions during the entire freeze–drying cycle. The high sensitivity of SXRD allowed us to monitor all the crystalline phases simultaneously. While DHPD crystallizes in frozen solution, it dehydrates *incompletely* during primary drying and *completely* during secondary drying. The impact of initial solute concentration on the phase composition during the entire freeze–drying cycle was quantified.

KEY WORDS: disodium hydrogen phosphate dodecahydrate; glycine; *in situ* freeze–drying; phase transitions; phosphate buffer; synchrotron X-ray diffraction.

INTRODUCTION

Lyophilization (freeze–drying) is widely utilized for manufacturing pharmaceutical proteins, diagnostic agents and other thermolabile agents. Freeze–dried formulations are multi-component systems containing the active pharmaceutical ingredient (API) and excipients such as bulking agents, lyoprotectants and buffers. Lyophilization of aqueous solutions typically involves freezing, annealing and drying stages. During these stages, the API as well as the excipient can undergo phase transformations. The physical form of the formulation components in the final lyophiles can impact the product stability (chemical as well as physical) and performance (e.g., reconstitution time) (1–4). In protein formulations, a major challenge is to minimize the damage to API from the stresses (e.g., pH changes, increased solute concentration brought about by ice crystallization, dehydration) experienced during the freeze–drying. Amorphous sugars (e.g., sucrose, trehalose) provide lyoprotection during freeze–drying and subsequent storage. Crystalline bulking agents (e.g., glycine) enable primary drying at elevated temperatures and therefore decrease the cycle time and also result in elegant lyophiles (1,3–8).

When the prelyophilization solution is cooled, crystallization of ice is often the first event, accompanied by freeze concentration of solutes (3,8–10). Although solute (e.g., buffer salt) crystallization is possible, in many cases, it is

[1] Department of Pharmaceutics, College of Pharmacy, University of Minnesota, Minneapolis, Minnesota 55455, USA.
[2] *Present address*: sanofi-aventis, Pharmaceutical Sciences Department, Bridgewater, New Jersey 08807, USA.
[3] Department of Physics, Kent State University, Kent, Ohio 44242, USA.
[4] Pfizer Groton Laboratories, Groton, Connecticut 06340, USA.
[5] To whom correspondence should be addressed. (e-mail: dushamaya@gmail.com; surya001@umn.edu)

retained amorphous. Solute as well as ice crystallization from the freeze-concentrate can often be induced by annealing the frozen solutions (3,8–13). Pikal-Cleland *et al*. demonstrated a decrease in crystallization of disodium hydrogen phosphate buffer (initial concentration 10 mM) in the presence of amorphous glycine (initial concentration 50 mM). Interestingly, when the initial glycine concentration was ≥ 100 mM, the crystallization of buffer salt was facilitated (7). Pyne *et al*. demonstrated a complex interplay between the amorphous and crystalline phases in the ternary system composed of mannitol, glycine and sodium phosphate (14). The crystallization of buffer salts (e.g., in the case of sodium phosphate buffer) from the freeze-concentrate is not desired due to the potential for significant pH shifts that can affect the stability of API (7,9,15–19).

The possible phase transformation during primary drying are: the (a) solute crystallization from freeze-concentrate, (b) partial or complete dehydration of a hydrate, with the anhydrous phase being crystalline, partially crystalline or amorphous, (c) polymorphic transitions of solute (1–3,5,8, 11–13,20). Chatterjee *et al*. demonstrated the dehydration of raffinose pentahydrate to amorphous anhydrate during primary drying (5). The phase separated raffinose, although amorphous in the final lyophile, significantly influenced the protein activity. Secondary drying is the last stage where the unfrozen water is removed by desorption. No major phase transitions are expected at this stage. The goal is to achieve the target residual moisture content of the lyophile, generally > 1% *w/w* (1,3,8).

In this context, to develop a robust freeze–drying cycle, it is important to: (a) identify the major phase transitions of formulation components during the entire freeze–drying cycle and (b) quantify solid-state transitions at different stages of freeze–drying. Therefore, an approach based on characterization of final lyophile alone could be misleading. Although, new analytical methods are under development, it remains difficult to identify and quantify phase changes in complex multi-component systems that are relevant to pharmaceutical formulations.

In the case of glycine, the formulation components including the API can inhibit or enhance the crystallization of glycine during freezing (21–25). Moreover, the solution pH before lyophilization, can not only influence the extent of glycine crystallization, but might influence the salt and polymorphic forms of glycine. The isoelectric pH of glycine ($^{+}H_3NCH_2COO^{-}$) is 5.97. The p*K*a values of 2.35 (carboxylic acid) and 9.78 (amine), dictate the speciation and solubility of glycine as a function of pH (21–25). At ambient conditions, neutral glycine exists in three polymorphic forms, with the order of their thermodynamic stability being $\gamma > \alpha > \beta$ (26–29). In recent years, considerable attention has been paid to the process-induced phase transitions of glycine polymorphs (7,9, 20–36). Akers *et al*. demonstrated the effect of glycine salts, initial solution pH, and ionic strength on the glycine crystallization in frozen solutions and lyophiles (21). The effect of processing conditions (e.g., cooling rate, annealing) have been studied mostly in neutral glycine solutions. Earlier studies used thermal analysis and low-temperature X-ray diffractometry (XRD) to monitor the impact of an additive (sucrose) and processing conditions on glycine phase transformations during cooling and annealing (37,38). Chongprasert *et al*. utilized low-temperature differential scanning calorimetry (DSC) and freeze–drying microscopy to investigate the thermal behavior of glycine (22), while Pyne and Suryanarayanan used low-temperature (XRD) to study the phase transitions of glycine in frozen aqueous solutions and during freeze–drying (35). There has been no attempt to quantify the crystalline glycine content, during different stages of the freeze–drying cycle, both in the presence and absence of buffer. In our previous report, we have shown the crystallization behavior of glycine in frozen solutions and final lyophiles over the pH range of 1 to 10 (24).

It is known that the crystallization of the alkaline component of phosphate buffer as disodium hydrogen phosphate dodecahydrate (DHPD) causes pH shift in frozen solutions (9,15–18). Pronounced pH shift, up to 3 units, were observed when the initial buffer concentrations were ≥50 mM (15,16). In our previous report, using synchrotron X-ray diffractometry (SXRD), we have demonstrated the effect of initial solute concentration (ranging from 1 to 100 mM) on the selective crystallization of DHPD (19). Gomez *et al*. developed an elegant method to monitor pH changes at temperatures ≥ −20°C by using a low temperature electrode (15,16). Unfortunately, this approach will not be suitable to monitor the pH at the temperature of our interest (approximately −50°C), and also during drying. To this end, SXRD can be utilized for quantification of crystalline phases that are responsible for causing such pH-shifts (19,24). Alternative methods are being developed to monitor shift in acidity induced by freeze–drying. Govindarajan *et al*. utilized sulfonephthalein dyes and diffuse reflectance visible spectroscopy to evaluate the acidity of trehalose-citrate lyophiles (39).

We have demonstrated the utility and power of SXRD to detect crystallization of DHPD from sodium phosphate buffer solution (1.0 mM; pH 7.4 at 25°C) cooled to −50°C and annealed at −25°C (19,24). Synchrotron radiation has already shown promise for *in situ* monitoring of crystallization and for quantifying the crystallinity in a substantially amorphous matrix (40–42). In addition to high sensitivity, very rapid data collection is possible (<1 s) enabling time-resolved studies (19,24,40–42). An approach based on SXRD could offer numerous advantages. (1) Reliable, unambiguous and simultaneous detection of multiple solid phases crystallizing from solution. The high sensitivity enables detection of even minor formulation components such as buffer salts. (2) Quantification of analyte crystallinity in complex, multi-component systems. (3) Capability to monitor phase transitions during the entire freeze–drying cycle.

In this study we had two objectives. (1) To develop a synchrotron X-ray diffraction method to monitor phase transition during the entire freeze–drying cycle. Freeze–drying was carried out in the sample chamber of the X-ray diffractometer, and the sample was periodically exposed to synchrotron radiation. Aqueous sodium phosphate buffered glycine solutions (glycine to buffer molar ratios of 1:1, 1:3 and 3:1) were utilized as model systems. (2) To investigate the effect of initial solute concentration on the crystallization of glycine and phosphate buffer salt during lyophilization.

To our knowledge, this is the first report wherein the high sensitivity of SXRD was utilized to quantify crystalline phases (glycine, phosphate buffer salt and ice) during all the stages of freeze–drying. In addition, the influence of solute

concentration on phase transitions during the freeze–drying cycle was established.

MATERIALS AND METHODS

Materials

Glycine, disodium hydrogen phosphate (Na_2HPO_4) and monosodium dihydrogen phosphate (NaH_2PO_4) were obtained from Sigma (>99% purity), and used without further purification. The solutions were prepared with deionized water. A pH meter (Oakton), calibrated with standard buffer solutions (Oakton standard buffers; pH 1.68, 4.01, 7.00 and 10.00; certified by NIST) was used.

Preparation of Sodium Phosphate Buffered Solutions

The aqueous solutions containing glycine and phosphate buffer (glycine to buffer molar ratios of 1:1, 1:3 and 3:1; initial concentration (mM) ratios of 50:50, 17:50 and 50:17) were prepared by dissolving appropriate amounts of glycine and sodium phosphate buffer (Na_2HPO_4: NaH_2PO_4; 9:1 w/w ratio) in 50 ml deionized water. The final solution pH (7.4±0.01) was confirmed experimentally. All solutions were filtered (0.45 μm polyvinylidene fluoride filter) and stored in tightly closed scintillation vials in the dark, at room temperature (RT).

Methods

In Situ Freeze–Drying—Synchrotron XRD (Transmission Mode)

The experimental setup is shown in Fig. 1. The experiments were performed at the synchrotron beam line 6-ID-B of the Midwest Universities Collaborative Team's-Sector 6, at the Advanced Photon Source, Argonne National Laboratory (Argonne, IL, USA) (Fig. 1a). The variable temperature stage (High-Tran Cooling System, capable of controlled cooling by using liquid nitrogen) was attached to the Eulerian cradle (Huber 512) using an aluminum (Al) plate (Fig. 1b). Drying (both primary and secondary) was performed by attaching a vacuum pump to the sample stage. An X-ray beam (0.76534 Å; beam size 100 (vertical)×200 (horizontal) μm) was used, wherein the flux of the incident X-rays (intensity: 1,013 photons/s/mrad^2/mm^2) was attenuated to prevent detector saturation. The monochromator, a triple-bounce, channel-cut, [111] faces polished Si single crystal limited the line broadening to its theoretical low limit, i.e. the Darwin width. An image plate detector (Mar345) with 3,450×3,450 pixel resolution in 34.5 mm diameter area, with a readout time of 108 seconds (best resolution mode), was used. The sample to detector distance was set to 500.1 mm. The calibration was performed using a silicon standard (SRM 640b, NIST).

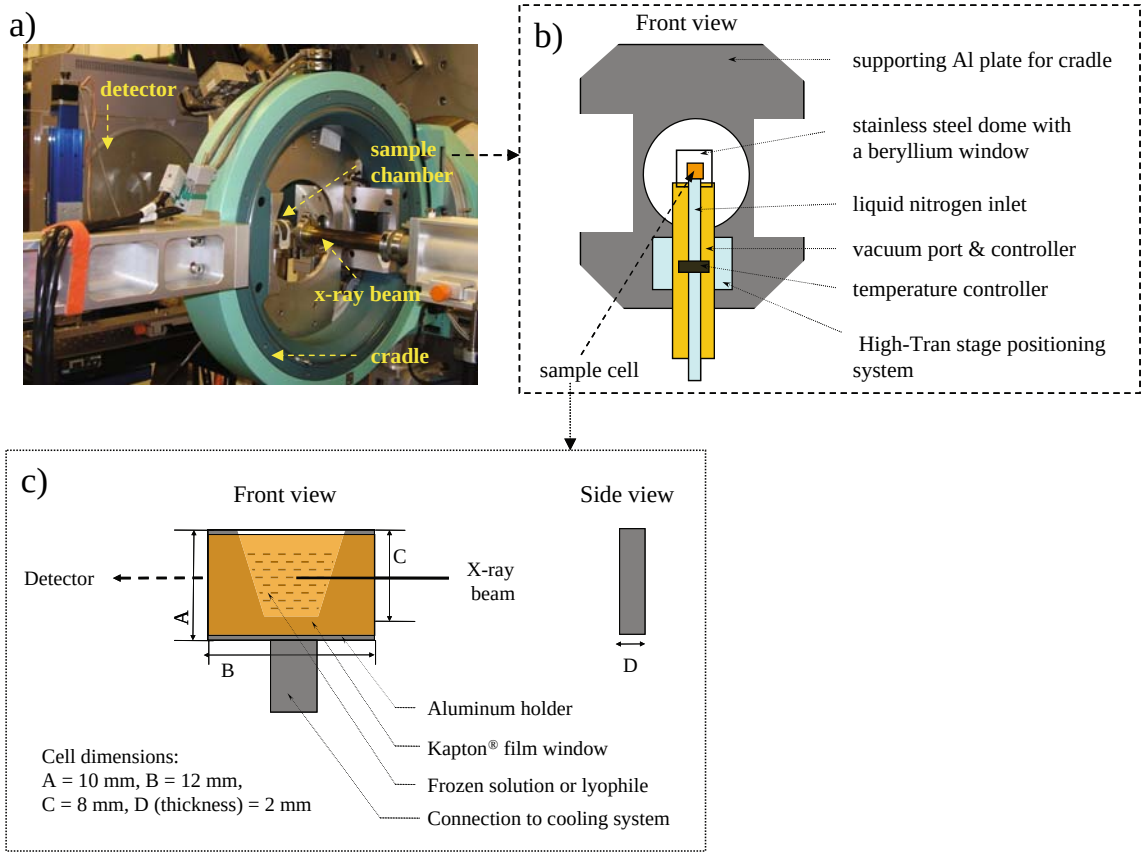

Fig. 1. Experimental setup for the freeze–drying process used at the synchrotron beamline, Advance Photon Source, Argonne National Laboratory IL, USA. **a**) The X-ray beam flight path, the Eulerian cradle and the two-dimensional image-plate (Mar345) detector. **b**) Schematic of the sample chamber (view from the source). **c**) Schematic of the custom-designed sample cell.

Sodium phosphate buffered glycine solution (200 μL) was placed in a custom-designed Al sample cell with a Kapton® window (Fig. 1c). The Al sample cell was designed to enable all the steps of the freeze–drying to be carried out in the beamline, while exposing a representative sample to the synchrotron beam. The sample cell was covered with a stainless steel dome with a beryllium window. The freeze–drying process parameters are provided in the "RESULTS" and "DISCUSSION" sections. Typically, the solutions were cooled, at 2°C/min, from RT to −50°C, held for 10 min, and heated at 5°C/min to the annealing temperature of −20°C. While the primary drying was conducted at −25°C under reduced pressure (100 mTorr), the secondary drying temperature ranged between 0 and 25°C. The freeze–drying conditions were based on the reported thermal transitions of glycine and phosphate buffer in frozen solutions (7,35). The buffered glycine solutions were exposed to high-intensity X-ray beam (total transmission: 3.44× 10−2 keV, exposure time: 5 or 10 s) during various stages of the freeze–drying cycle. Additionally, a blank or background reading was obtained by exposing an empty sample cell to the X-ray beam. Selected experiments were performed in duplicate.

XRD Data Analysis

Time-resolved two-dimensional (2D) data were integrated to yield one-dimensional (1D) d-spacing (Å) or 2θ (°) scans using the FIT2D software developed by A. P. Hammersley of the European Synchrotron Radiation Facility (43,44). The peak intensities were normalized to transmission, attenuation and exposure time of X-ray beam. These were imported using commercially available software (JADE version 7.1, Materials Data, Inc.) and a plot of the integrated intensity (counts) as a function of d-spacing (Å) was obtained in each case. The results were compared with the published data in the Powder Diffraction Files (PDF) of the International Centre for Diffraction Data (ICDD). All the relevant 1D-XRD patterns were overlaid and compared with the standard stick patterns of crystalline glycine phases, sodium phosphate buffer and hexagonal ice (33). This formed the basis for the assignment of major and minor phases at different stages of the freeze–drying cycle.

RESULTS

The 'as is' glycine (anhydrous α-form) and sodium phosphate buffer components (anhydrous Na_2HPO_4 and NaH_2PO_4) were identified by XRD, DSC and thermogravimetric analysis.

We had earlier shown that glycine crystallization (initial concentration 267 mM) in frozen solutions was inhibited when the initial sodium phosphate buffer concentration was high (200 mM) (24). This was attributed to the pH shift brought about by the selective crystallization of disodium hydrogen phosphate dodecahydrate (DHPD) (15,16). We observed that, upon annealing, a considerable fraction of glycine crystallized (24). In this report, we evaluated the effect of a pharmaceutically relevant sodium phosphate buffer concentration (50 mM and 17 mM) on glycine crystallization during the entire freeze–drying cycle. The high sensitivity of SXRD enabled us to study crystallization from solutions with low initial solute concentrations [glycine to sodium phosphate buffer ratios were 1:1 (50:50 mM), 1:3 (17:50 mM) and 3:1 (50:17 mM)]. Additionally, we evaluated the utility of SXRD to quantify phase transitions during all stages of the freeze–drying cycle.

Further, it is known that the crystallization of DHPD is influenced by the glycine concentration (7,24). Pikal-Cleland *et al*. reported that, both in 10 and 100 mM phosphate buffered glycine (glycine concentration ≥ 100 mM), pH shift due to DHPD crystallization was unavoidable (7). In our study, initial compositions were selected to understand the effect of glycine concentration on buffer salt crystallization and *vice versa*. The extent of glycine and DHPD crystallization, during the freeze–drying of solutions of different compositions, was determined.

Equimolar Ratio of Glycine to Phosphate Buffer (50 mM)

Fig. 2 contains representative two-dimensional SXRD patterns, obtained during the various stages of lyophilization cycle. Fig. 3 is the plot of the integrated intensities of characteristic lines of β-glycine, DHPD and ice, as a function of freeze–drying conditions (temperature and time) for 1:1 glycine–phosphate buffer system.

Solute Crystallization During Cooling. Crystallization of hexagonal ice, β-glycine and DHPD were first observed at −30°C, with no appreciable increase in the peak intensities after cooling to −50°C and holding for 10 min (Figs. 2 and 3). As expected, none of the characteristic peaks of monosodium hydrogen phosphate were observed, which is known to remain amorphous even at a high concentration (11,12).

Effect of Annealing. After holding at −50°C for 10 min, the frozen solutions were heated to −20°C and annealed for 30 min. Both DHPD and glycine peak intensities were essentially unchanged (Fig. 3). We had earlier observed that, in the absence of glycine, DHPD readily crystallized on cooling, from solutions of initial concentration ranging from 10 to 100 mM, and annealing did not facilitate further solute crystallization (19). Interestingly, the presence of glycine, at an initial concentration of 50 mM, did not influence DHPD crystallization in frozen systems.

Phase Transitions during Primary Drying: Extent of Solute Crystallization and Incomplete Dehydration of DHPD. The solution annealed at −20°C, was cooled to −25°C and dried under vacuum (100 mTorr) for 90 min. As the intensities of the characteristic lines of ice decreased, there was an increase in the intensities of the characteristic lines of both β-glycine and DHPD (Fig. 3). After ~30 min, the ice peaks had essentially disappeared, indicating that sublimation was almost complete (Fig. 3). The decrease in the intensities of the ice peaks was accompanied by the appearance and increase in the intensity of several characteristic peaks of β-glycine and DHPD. While the DHPD peak intensities were unaffected by annealing, a pronounced increase was observed during the first 30 min of primary drying (Fig. 3). Disodium hydrogen phosphate is known to crystallize spontaneously as the least soluble dodecahydrate (DHPD). Upon ice sublimation, the amorphous Na_2HPO_4 crystallizes as DHPD from the freeze-concentrate. A similar but less pronounced effect was observed for glycine crystallization (Fig. 3). Upon continuing the primary drying from 45 to 90 min, the remaining ice sublimed. There was also a pronounced decrease in the intensities of the DHPD peaks. This can be explained by the collapse of crystal lattice caused by

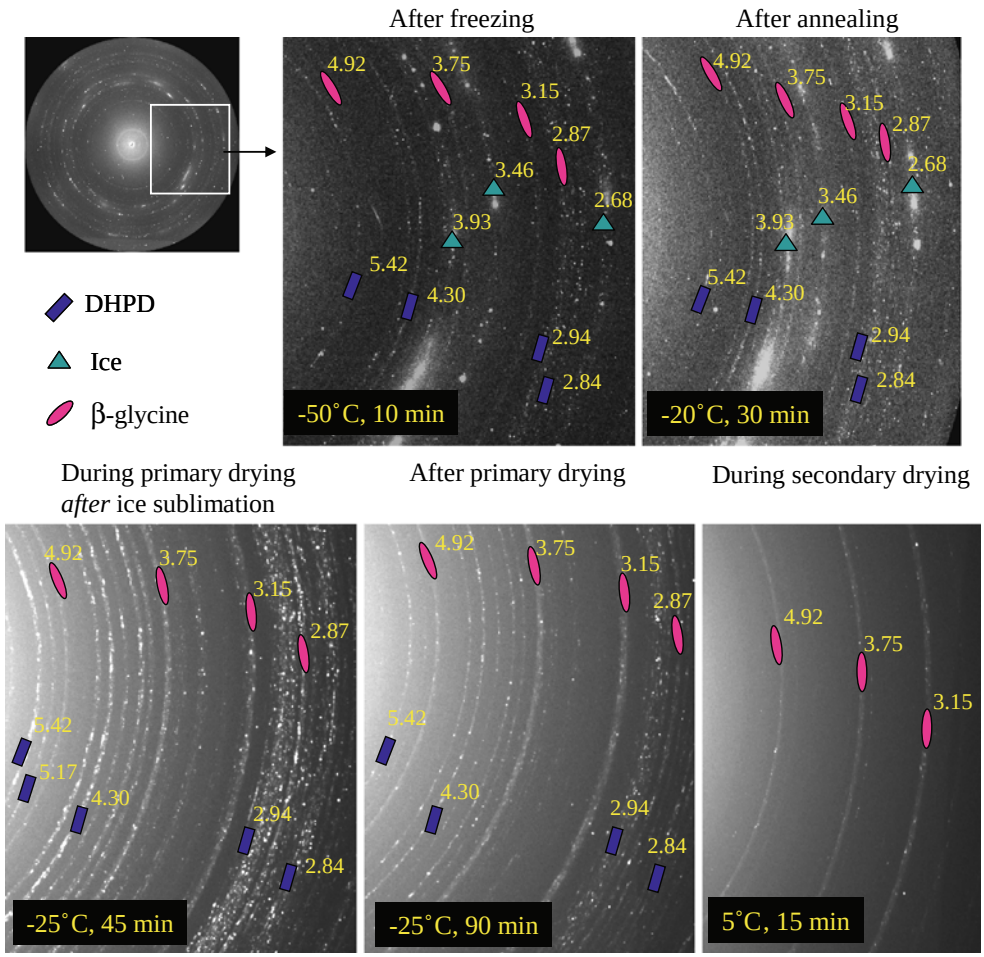

Fig. 2. Representative 2D-SXRD patterns of aqueous glycine (50 mM)—sodium phosphate (50 mM) buffer solution (initial pH 7.4) at different stages of the freeze–drying cycle. The solutions were cooled at 2°C/min from RT to −50°C, held for 10 min, then heated at 5°C/min to −20°C and annealed for 30 min. Primary drying was conducted at −25°C under vacuum (100 mTorr) for 90 min. Secondary drying was conducted under vacuum (100 mTorr) at 0°C for 10 min and at 5°C for 15 min. Characteristic d-spacing (Å) lines of β-glycine, DHPD and ice are shown.

dehydration, resulting in amorphous disodium hydrogen phosphate (Fig. 3). The glycine peak intensities, as expected, were essential unchanged during the later stages of primary drying.

Phase Transitions during Secondary Drying: Complete Dehydration of DHPD. To investigate any further phase transformations at higher temperatures, the lyophiles after primary drying were heated at 5°C/min under vacuum (100 mTorr) to 0°C and held for 20 min. While the intensities of the β-glycine peaks were essentially unchanged, no new peaks appeared. This indicates complete dehydration of DHPD to amorphous Na_2HPO_4 (Figs. 2 and 3). Further drying of the lyophiles, first at 5°C and then at 25°C, caused no detectable changes in the XRD pattern.

Higher Buffer Concentration (Glycine:Phosphate Buffer::17: 50 mM)

A plot of the intensities of the characteristic peaks of DHPD and ice, during various stages of freeze–drying, is presented in Fig. 4. As observed earlier (equimolar ratio of glycine to buffer), the crystallization of DHPD and ice was evident at −30°C (Fig. 4). There was no evidence of glycine crystallization. Upon annealing at −20°C for 30 min there was no significant change in the extent of DHPD crystallization. During primary drying at −25°C, there was a pronounced increase in the intensity of DHPD peaks during the first 10 min (Fig. 4). At 12 min, rapid sublimation of ice was evident from the dramatic decrease in the intensity of ice peaks. At this time, the DHPD peak intensity was the maximum. Upon further drying, when the remaining ice sublimed, the dehydration of DHPD yielded amorphous Na_2HPO_4 (Fig. 4). At the end of primary drying, based on the intensities of DHPD peaks, approximately 50% of the crystallized DHPD had dehydrated. The dehydration was complete after secondary drying at 0°C. The lyophile was X-ray amorphous even when the secondary drying temperature was progressively increased to 25°C (Fig. 4).

Complete Inhibition of Glycine Crystallization—Impact of DHPD Crystallization and Dehydration. There was no evidence of glycine crystallization during the different stages of freeze–drying cycle (Fig. 4). Glycine remained amorphous

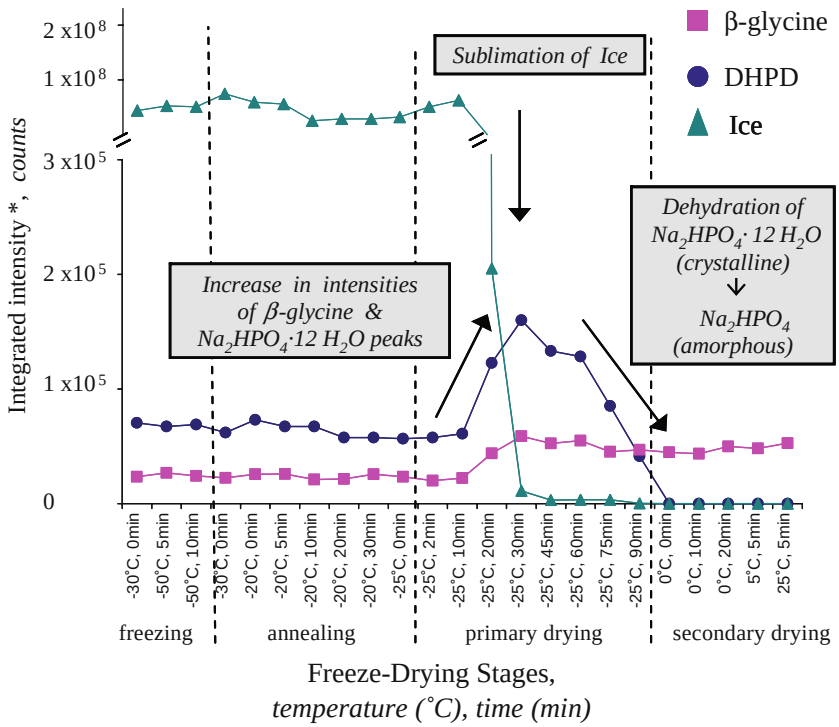

Fig. 3. The integrated intensity (counts) of some characteristic peaks of β-glycine, disodium hydrogen phosphate dodecahydrate (DHPD) and ice at different stages of the freeze–drying cycle. *Sum of the intensities of: i) the 4.92 and 3.15 Å lines of β-glycine, ii) 5.42 and 4.30 Å lines of DHPD, and iii) 3.93, 3.43 and 2.68 Å lines of ice. *The initial glycine to sodium phosphate buffer ratio was 1:1 (50:50 mM).* The freeze–drying conditions are described in the legend of Fig. 2.

not only in frozen solutions but also in the final lyophile. This inhibition of glycine crystallization can be explained based on previous reports (22). The solute concentration, pH and phase composition changes during the entire freeze–drying process can influence the resulting solid state of glycine. In our previous report, when the glycine to buffer ratio was ~1.3:1 (267:200 mM actual initial concentration) a significant fraction of glycine remained amorphous in the freeze-concentrate and crystallized upon annealing (24). The inhibition of glycine crystallization could be attributed to an acidic pH shift caused by the DHPD crystallization. In the current study, the concentration of sodium phosphate buffer (50 mM) was significantly higher than that of glycine (17 mM). This high initial buffer concentration, coupled with the pH-shift due to buffer salt crystallization, would have caused complete inhibition of glycine crystallization in the frozen system. Interestingly, glycine was retained amorphous in the final lyophile. It is possible that DHPD crystallization during drying further inhibited glycine crystallization.

Lower Buffer Concentration (Glycine:Phosphate Buffer:: 50:17 mM)

Fig. 5 contains representative two-dimensional SXRD patterns, obtained during the various stages of the lyophilization cycle. From these patterns, the intensities of the characteristic peaks of β-glycine, DHPD and ice were obtained and plotted (Fig. 6). When cooled to −50°C, only the crystallization of ice was observed. The β-glycine crystallization was evident after holding at −50°C for 10 min, though there was no evidence of DHPD crystallization (Figs. 5 and 6). Gomez *et al.* observed a pH shift of ~2 units from a solution buffered to pH 7.4. In this system the initial buffer salt concentration was 8 mM. However, when the initial buffer concentration was 100 mM the pH shift was much higher (~3.2 units) (15,16). The less pronounced pH-shift, at low initial buffer concentration, is attributable to the decrease in DHPD crystallization at far-from equilibrium conditions (7,15,16). In our system, the low initial buffer concentration (17 mM) and the presence of glycine substantially delayed the crystallization of DHPD.

Upon annealing the frozen solutions at −20°C, the crystalline β-glycine content increased continuously as a function of time (Fig. 6). Although crystallization of DHPD was not evident during freezing, the characteristic peaks of DHPD (including the 5.42 Å peak) were observed after 30 min of annealing at −20°C, with a pronounced increase in intensity as annealing progressed (Figs. 5 and 6). Interestingly, contrary to expectations, the intensity of ice peaks decreased during annealing. We did not attempt to investigate this further, since this paper focused on phase transitions of solutes.

The increase in the crystalline DHPD content continued during primary drying at −25°C until a significant fraction of the ice had sublimed (Fig. 6). The crystalline DHPD content appeared to be much higher than that in the other two

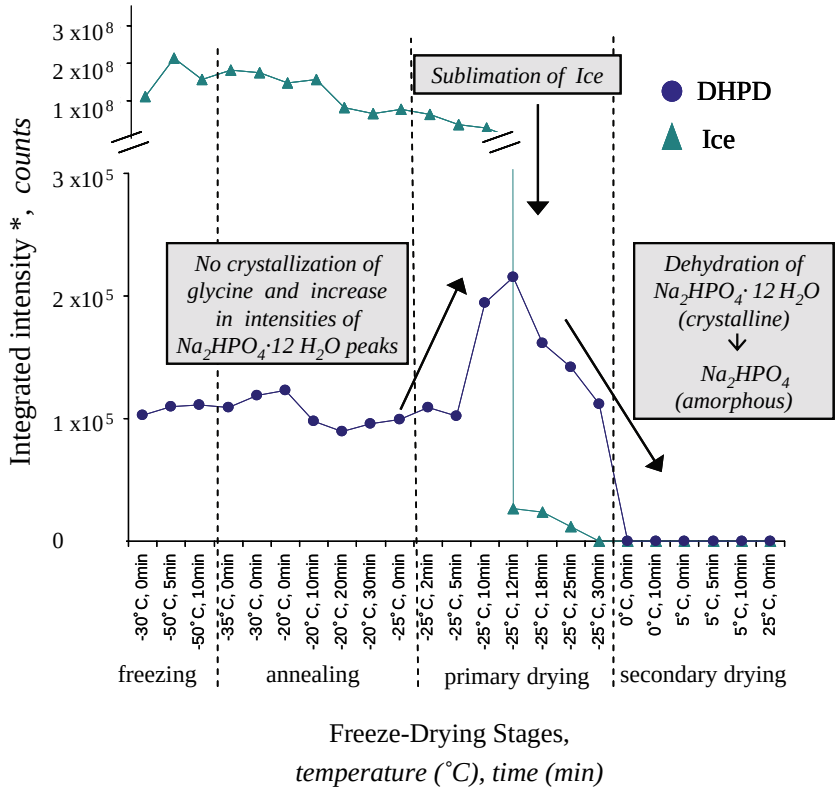

Fig. 4. The integrated intensity (counts) of some characteristic peaks of disodium hydrogen phosphate dodecahydrate (DHPD) and ice at different stages of the freeze–drying cycle. No peaks of any forms of glycine were observed. *Sum of the intensities of: i) the 4.92 and 3.15 Å lines of β-glycine, ii) 5.42 and 4.30 Å lines of DHPD, and iii) 3.93, 3.43 and 2.68 Å lines of ice. *The initial glycine to sodium phosphate buffer ratio was 1:3 (17:50 mM).*

compositions. This observation is noteworthy in light of the fact that the initial buffer concentration of 17 mM, is much lower than in the other two cases (50 mM). Dehydration of DHPD was initiated only when the ice sublimation was almost complete (Fig. 6). The crystallization of β-glycine progressed during primary drying and leveled off during secondary drying (Fig. 6). Only crystalline β-glycine was detected in the final lyophile indicating the complete dehydration of DHPD (Fig. 6).

DISCUSSION

Effect of Prelyophilization Solution Composition on Phase Transitions During Lyophilization

In the solutions cooled to −50°C, crystalline hexagonal ice was the major component. When the initial phosphate buffer concentration (50 mM) was significantly higher than that of glycine (17 mM), only DHPD crystallization was observed (Fig. 4). In contrast, at a higher initial glycine concentration (50 mM), only crystallization of β-glycine was evident (Fig. 6). When the initial concentrations of glycine and buffer salts were equal (50 mM each), crystallization of both DHPD and β-glycine was observed (Fig. 3). In all cases, there was no evidence of crystallization of monosodium dihydrogen phosphate.

Annealing facilitated further crystallization of glycine in 3:1 (glycine:buffer) system (Fig. 6) but not in 1:1 system (Fig. 3). It is possible that in 1:1 system, both glycine and DHPD crystallization was completed during cooling. When the initial sodium phosphate buffer concentration was higher (1:3), glycine remained amorphous even at the end of annealing (Fig. 4). The possible reasons for this observation were discussed earlier. There was no pronounced effect of annealing on DHPD crystallization in both 1:1 and 3:1 (glycine: buffer) systems (Figs. 3 and 6). Interestingly, when the glycine concentration was higher (3:1 system, Fig. 6) DHPD crystallization became evident only towards the end of annealing.

During the initial stage of primary drying, there was ice sublimation, evident from the decrease in the intensities of the characteristic hexagonal ice peaks, and a concomitant increase in the intensities of peaks attributed to β-glycine and DHPD. When the initial buffer concentration was high (1:3 system), DHPD constituted the major crystalline component (Fig. 4). In all cases, towards the latter part of primary drying, as ice sublimation was complete, (evidenced by the disappearance of the ice peaks) there was also a concomitant decrease in the DHPD peak intensities, revealing dehydration of DHPD to amorphous Na_2HPO_4. Such a crystalline hydrate → amorphous anhydrate transition of the sodium phosphate buffer salt was reported earlier (34). As discussed earlier, there was no evidence of glycine crystallization when the initial glycine concentration was 17 mM (Fig. 4).

At all compositions, the dehydration of DHPD, leading to the formation of amorphous Na_2HPO_4 was complete during secondary drying. Thus, in the final lyophile, both the buffer components (Na_2HPO_4 and NaH_2PO_4) were

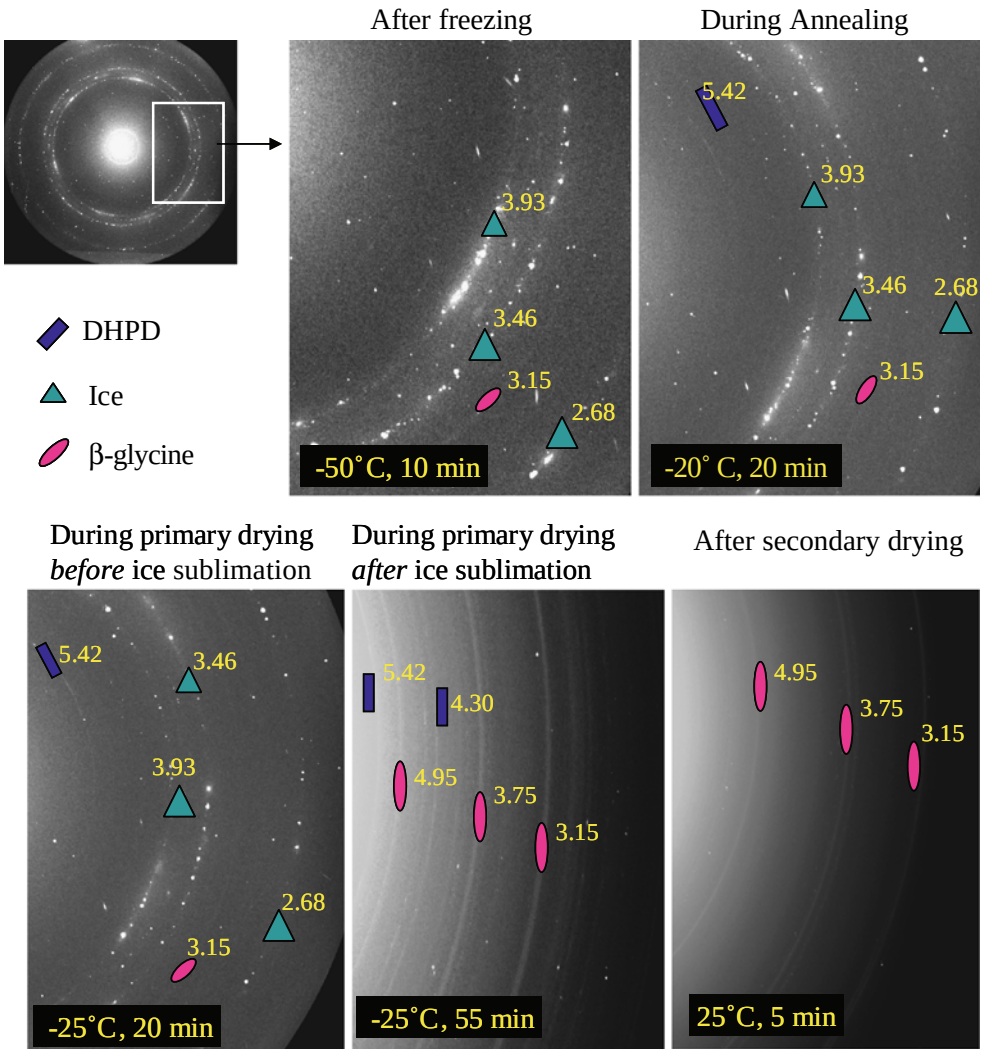

Fig. 5. Representative 2D-SXRD patterns of aqueous glycine (50 mM)—sodium phosphate (17 mM) buffer solution (initial pH 7.4) at different stages of the freeze–drying cycle. Characteristic d-spacing (Å) lines of β-glycine, DHPD and ice are shown. The freeze–drying conditions are described in the legend of Fig. 2.

amorphous. However, since the disodium hydrogen phosphate had crystallized as a dodecahydrate, and then underwent a crystalline hydrate → amorphous anhydrate transition, it is expected to exist as a discrete phase, formed only after a significant fraction of the ice had sublimed in the final lyophile. The final lyophile, prepared from the 1:1 or 3:1 systems, contained β-glycine. At a high buffer concentration (3:1), glycine was retained amorphous (Fig. 4).

To our knowledge, *crystallization of DHPD followed by its incomplete dehydration during primary drying* has not been previously reported (15,16,34,35). We believe that the capability of *in situ* SXRD to acquire time-resolved data, coupled with its high sensitivity revealed this phase transition during processing.

Effect of Initial Solute Concentration on the Crystallization of Glycine and Phosphate Buffer in Freeze–Dried Systems

The crystallization behavior of glycine and DHPD can be influenced by the initial solute concentration as well as the processing conditions. In this study, while keeping the processing conditions (temperature and pressure) fixed, the solute concentrations were varied. This design of experiment enabled us to determine the effect of concentration and understand the effect of one solute on the crystallization behavior of the other.

Effect of Phosphate Buffer Concentration on Glycine Crystallization

The extent of glycine crystallization, during all stages of the freeze–drying process, was affected by the sodium phosphate buffer concentration (Fig. 7). At the higher buffer concentration (50 mM), there was a substantial inhibition of glycine crystallization. When these solutions were cooled, disodium hydrogen phosphate crystallized as the dodecahydrate (DHPD) which is known to cause a significant acidic pH shift (15,16). This shift in pH alters the speciation of glycine and inhibits glycine crystallization (5,21,24). In our previous study, when glycine solutions (267 mM initial

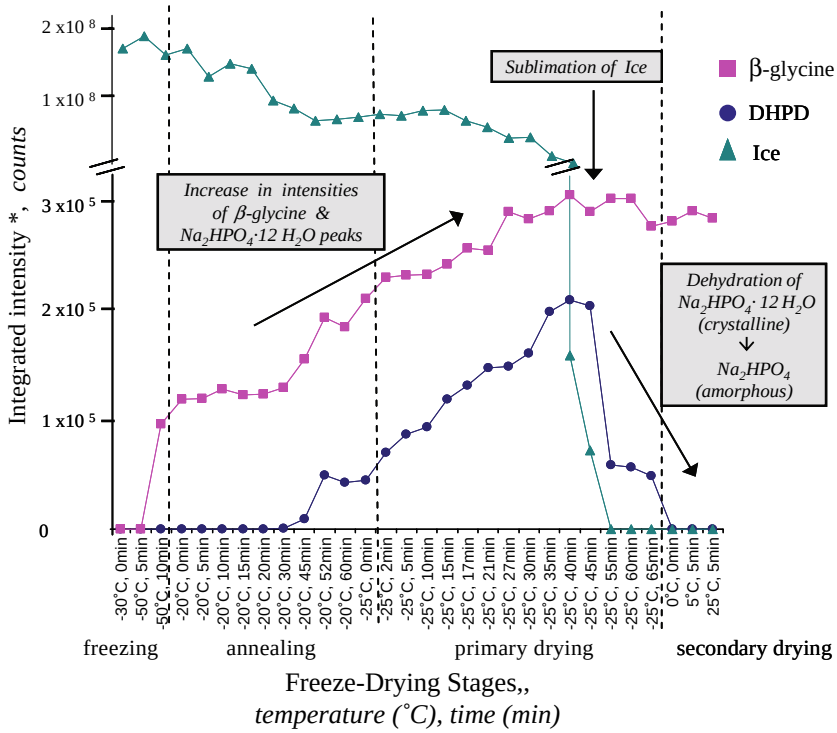

Fig. 6. The integrated intensity (counts) of some characteristic peaks of β-glycine, disodium hydrogen phosphate dodecahydrate (DHPD) and ice at different stages of the freeze–drying cycle. *Sum of the intensities of: i) the 4.92 and 3.15 Å lines of β-glycine, ii) 5.42 and 4.30 Å lines of DHPD, and iii) 3.93, 3.43 and 2.68 Å lines of ice. *The initial glycine to sodium phosphate buffer ratio was 3:1 (50:17 mM).*

concentration) adjusted to pH 3 or buffered to pH 7.4 (200 mM sodium phosphate buffer), were cooled to −50°C, a significant fraction of glycine remained amorphous. In the present case, when the initial concentration of phosphate buffer and glycine were the same (50 mM each), a more

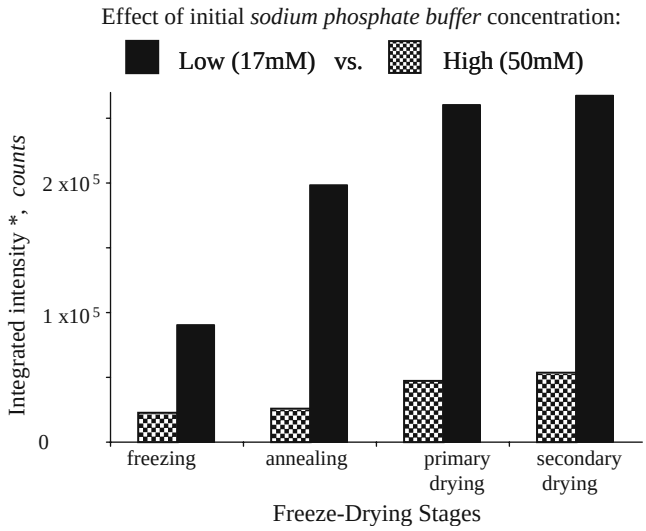

Fig. 7. Effect of buffer concentration on glycine crystallization during various stages of lyophilization. While the glycine concentration in the prelyophilization solution was 50 mM, the buffer concentration was either 17 or 50 mM. *Sum of the integrated intensities of the 4.92 and 3.15 Å lines of β-glycine (35).

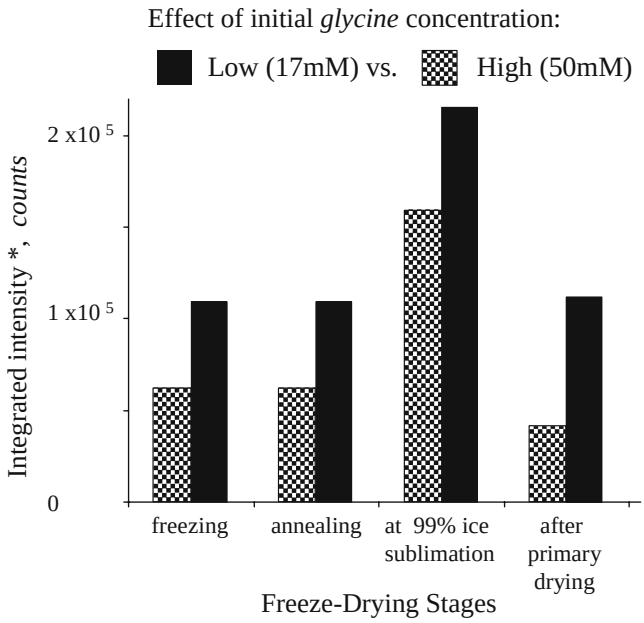

Fig. 8. Effect of glycine concentration on the DHPD crystallization during different stages of lyophilization. While the buffer concentration in the prelyophilization solution was 50 mM, the glycine concentration was either 17 or 50 mM. *Sum of the integrated intensities of the 5.42 and 4.30 Å lines of DHPD (35). The DHPD line intensities, after freezing and annealing, as well as after substantial (~99%) and complete ice sublimation, are reported.

pronounced inhibition of glycine crystallization was observed. This was attributed to the pH shifts in the freeze–concentrate.

At ambient conditions, inhibition of α-glycine crystallization in solutions with initial pH values of 3 or 9 was explained to occur via 'self-poisoning' mechanism to produce γ-glycine (23). A crystal packing examination of α-glycine indicates that the hydrogen-bonded cyclic dimer (packed in two-dimensional array) is the building-block for the growth of α-glycine. The charged species of glycine inhibit the formation of the α-glycine dimers and consequently thermodynamically stable γ-glycine crystallizes in one-dimension polar chains (23,36). Interestingly, β-glycine exists as hydrogen-bonded monomers, which is known to crystallize rapidly in the presence of ice (21–23,25). There are no reports in the literature to suggest the inhibition of β-glycine (zwitterion) crystallization by charged glycine species ($^{+}H_3NCH_2COOH$ or $NH_2CH_2COO^{-}$).

Effect of Glycine Concentration on DHPD Crystallization and Dehydration

When the glycine concentration was increased from 17 to 50 mM, there was a small but consistent inhibitory effect on DHPD crystallization (Fig. 8). A higher glycine:buffer ratio in the prelyophilization solution is expected to result in a higher glycine concentration in the amorphous freeze-concentrate. The uncrystallized glycine is known to inhibit DHPD crystallization (7).

Significance and Practical Implications

Using sodium phosphate buffered glycine as a model system; we have demonstrated the utility and sensitivity of synchrotron radiation to monitor phase transformations during all the stages of the freeze–drying cycle. This approach will enable us to optimize the processing conditions as well as the formulation composition so as to obtain a robust lyophilized product. For example, our real time simulation studies can enable the optimization of the annealing conditions (temperature and time) to cause complete crystallization of the bulking agent (3,5,13,20,30). In addition to the phase behavior of the individual solutes, the effect of one solute on the crystallization behavior of others can be evaluated in complex multi-component systems of pharmaceutical interest. The SXRD method will be an excellent complement to the other techniques such as freeze–drying microscopy and DSC which are used to characterize frozen systems and to select critical process parameters. However, the unique feature of the XRD technique is that the system is monitored continuously, in real time, over the entire freeze–drying cycle. The high sensitivity of SXRD coupled with rapid data collection (time intervals<1 s), will also enable kinetic studies of physical and chemical processes during freeze–drying (ice sublimation, solute crystallization, dehydration, polymorphic transformation). Such studies, in addition to improving our understanding of the freeze–drying process, may enable process optimization with minimal batch-to-batch variability. Our model compositions did not contain an active pharmaceutical ingredient (API). The concentration and the physical form of the API can influence the phase behavior of the excipients and *vice versa*.

CONCLUSIONS

A high-intensity X-ray diffraction method was developed to monitor the phase transitions during the entire freeze–drying cycle of sodium phosphate buffered glycine solutions. The high sensitivity of SXRD provided quantitative information of the crystalline DHPD and β-glycine phases during the various stages of freeze–drying. The crystallization of DHPD followed by its incomplete dehydration during primary drying and complete dehydration during secondary drying was revealed. The impact of initial concentrations of phosphate buffer and glycine on the crystallization behavior of these two solutes, during the entire freeze–drying cycle, was quantified.

ACKNOWLEDGEMENT

The authors thank Dr. Douglas Robinson for the beamline management and support during the experiments. This work was supported, in part, by a Research Challenge award from the Ohio Board of Regents. Use of the Advanced Photon Source at Argonne National Laboratory was supported by the U. S. Department of Energy, Office of Science, Office of Basic Energy Sciences, under Contract No. W-31-109-Eng- 38. The Midwest Universities Collaborative Access Team (MUCAT) sector at the APS is supported by the U.S. Department of Energy, Basic Energy Sciences, Office of Science, through the Ames Laboratory under Contract No. W-7405-Eng-82. We thank Linda Sauer for her assistance in setting up the instrumentation.

REFERENCES

1. M. J. Pikal. Freeze Drying. In J. Swarbrickand, and J. C. Boylan (eds.), *Encyclopedia of Pharmaceutical Technology*, Marcel Dekker, , New York, 2002, pp. 1299–1326.
2. J. F. Carpenter, M. J. Pikal, B. S. Chang, and T. W. Randolph. Rational design of stable lyophilized protein formulations: some practical advice. *Pharm. Res*. **14**:969–975 (1997). doi:10.1023/A:1012180707283.
3. X. Tang, and M. J. Pikal. Design of freeze–drying processes for pharmaceuticals: practical advice. *Pharm. Res*. **21**:191–200 (2004). doi:10.1023/B:PHAM.0000016234.73023.75.
4. L. A. Trissel. Handbook of injectable drugs. ASHP, Bethesda, MD, 1994.
5. K. Chatterjee, E. Y. Shalaev, and R. Suryanarayanan. Raffinose crystallization during freeze–drying and its impact on recovery of protein activity. *Pharm. Res*. **22**:303–309 (2005). doi:10.1007/s11095-004-1198-y.
6. X. Liao, R. Krishnamurthy, and R. Suryanarayanan. Influence of the active pharmaceutical ingredient concentration on the physical state of mannitol—implications in freeze–drying. *Pharm. Res.* **22**:1978–1985 (2005). doi:10.1007/s11095-005-7625-x.
7. K. A. Pikal-Cleland, J. L. Cleland, T. J. Anchordoquy, and J. F. Carpenter. Effect of glycine on pH changes and protein stability during freeze–thawing in phosphate buffer systems. *J. Pharm. Sci.* **91**:1969–1979 (2002). doi:10.1002/jps.10184.
8. T. W. Randolph. Phase separation of excipients during lyophilization: effects on protein stability. *J. Pharm. Sci.* **86**:1198–1203 (1997). doi:10.1021/js970135b.
9. E. Y. Shalaev. The impact of buffer on processing and stability of freeze–dried dosage forms, part 1: solution freezing behavior. *Am. Pharm. Rev*. **8**:80–87 (2005).
10. E. Y. Shalaev, F. Franks, and P. Echlin. Crystalline and amorphous phases in the ternary system water-sucrose-sodium chloride. *J. Phy. Chem.* **100**:1144–1152 (1996). doi:10.1021/jp951052r.

11. R. K. Cavatur, and R. Suryanarayanan. Characterization of frozen aqueous solutions by low temperature X-ray powder diffractometry. *Pharm. Res.* **15**:194–199 (1998). doi:10.1023/A:1011950131312.
12. R. K. Cavatur, and R. Suryanarayanan. Characterization of phase transitions during freeze–drying by *in situ* X-ray powder diffractometry. *Pharm. Dev. Technol*. **3**:579–586 (1998). doi:10.3109/10837459809028642.
13. J. A. Searles, J. F. Carpenter, and T. W. Randolph. Annealing to optimize the primary drying rate, reduce freezing-induced drying rate heterogeneity, and determine Tg' in pharmaceutical lyophilization. *J. Pharm. Sci*. **90**:872–887 (2001). doi:10.1002/jps.1040.
14. A. Pyne, K. Chatterjee, and R. Suryanarayanan. Solute crystallization in mannitol-glycine systems - implications on protein stabilization in freeze–dried formulations. *J. Pharm. Sci*. **92**:2272–2283 (2003). doi:10.1002/jps.10487.
15. G. Gomez. Crystallization related pH changes during freezing of sodium phosphate buffer solutions. Ph.D. dissertation, *Department of Pharmaceutics*, University of Michigan, Ann Arbor, 1995, p. 188.
16. G. Gomez, M. J. Pikal, and N. Rodriguez-Hornedo. Effect of initial buffer composition on pH changes during far-from-equilibrium freezing of sodium phosphate buffer solutions. *Pharm. Res*. **18**:90–97 (2001). doi:10.1023/A:1011082911917.
17. L. van den Berg. pH changes in buffers and foods during freezing and subsequent storage. *Cryobiol*. **3**:236–242 (1966). doi:10.1016/S0011-2240(66)80017-2.
18. L. van den Berg, and D. Rose. Effect of freezing on the pH and composition of sodium and potassium phosphate solutions: the reciprocal system KH_2PO_4–Na_2HPO_4–H_2O. *Arch. Biochem. Biophys*. **81**:319–329 (1959). doi:10.1016/0003-9861(59)90209-7.
19. D. B. Varshney, S. Kumar, E. Y. Shalaev, S.-W. Kang, L. A. Gatlin, and R. Suryanarayanan. Solute crystallization in frozen systems-use of synchrotron radiation to improve sensitivity. *Pharm. Res*. **23**:2368–2374 (2006). doi:10.1007/s11095-006-9051-0.
20. K. Chatterjee, E. Y. Shalaev, and R. Suryanarayanan. Partially crystalline systems in lyophilization: II. Withstanding collapse at high primary drying temperatures and impact on protein activity recovery.. *J. Pharm. Sci*. **94**:809–820 (2005). doi:10.1002/jps.20304.
21. M. J. Akers, N. Milton, S. R. Byrn, and S. L. Nail. Glycine crystallization during freezing: the effect of salt form, pH, and ionic strength. *Pharm. Res.* **12**:1457–1461 (1995). doi:10.1023/A:1016223101872.
22. S. Chongprasert, S. A. Knopp, and S. L. Nail. Characterization of frozen solutions of glycine. *J. Pharm. Sci.* **90**:1720–1728 (2001). doi:10.1002/jps.1121.
23. C. S. Towler, R. J. Davey, R. W. Lancaster, and C. J. Price. Impact of molecular speciation on crystal nucleation in polymorphic systems: The conundrum of γ-glycine and molecular "self poisoning". *J. Am. Chem. Soc.* **126**:13347–13353 (2004). doi:10.1021/ja047507k.
24. D. B. Varshney, S. Kumar, E. Y. Shalaev, P. Sundaramurthi, S.-W. Kang, L. A. Gatlin, and R. Suryanarayanan. Glycine crystallization in frozen and freeze–dried systems: effect of pH and buffer concentration. *Pharm. Res*. **24**:593–604 (2007). doi:10.1007/s11095-006-9178-z.
25. L. Yu, and K. Ng. Glycine crystallization during spray drying: the pH effect on salt and polymorphic forms. *J. Pharm. Sci*. **91**:2367–2375 (2002). doi:10.1002/jps.10225.
26. E. V. Boldyreva, V. A. Drebushchak, T. N. Drebushchak, I. E. Paukov, Y. A. Kovalevskaya, and E.S. Shutova. Polymorphism of glycine - thermodynamic aspects. Part 1. relative stability of polymorphs. *J. Therm. Anal. Cal.* **73**:409–418 (2003). doi:10.1023/A:1025405508035.
27. E. S. Ferrari, R. J. Davey, W. I. Cross, A. L. Gillon, and C. S. Towler. Crystallization in polymorphic systems: the solution-mediated transformation of β to α glycine. *Cryst. Growth Des.* **3**:53–60 (2003). doi:10.1021/cg025561b.
28. G. L. Perlovich, L. K. Hansen, and A. Bauer-Brandl. The polymorphism of glycine—thermochemical and structural aspects. *J. Therm. Anal. Cal.* **66**:699–715 (2001). doi:10.1023/A:1013179702730.
29. H. Sakai, H. Hosogai, T. Kawakita, K. Onuma, and K. Tsukamoto. Transformation of α-glycine to γ-glycine. *J. Cryst. Growth.* **116**:421–426 (1992). doi:10.1016/0022-0248(92)90651-X.
30. K. Chatterjee, E. Y. Shalaev, and R. Suryanarayanan. Partially crystalline systems in lyophilization: I. Use of ternary state diagrams to determine extent of crystallization of bulking agent. *J. Pharm. Sci.* **94**:798–808 (2005). doi:10.1002/jps.20303.
31. T. D. Davis, G. E. Peck, J. G. Stowell, K. R. Morris, and S. R. Byrn. Modelling and monitoring of polymorphic transformations during the drying phase of wet granulation. *Pharm. Res*. **21**:860–866 (2004). doi:10.1023/B:PHAM.0000026440.00508.cf.
32. X. Li, and S. L. Nail. Kinetics of glycine crystallization during freezing of sucrose/glycine excipient systems. *J. Pharm. Sci.* **94**:625–631 (2005). doi:10.1002/jps.20286.
33. Powder Diffraction File. hexagonal ice, card#00-042-1142; disodium hydrogen phosphate dodecahydrate, card#00-011-0657; α-glycine, card#00-032-1702; β-glycine, card#00-002-0171; γ-glycine, card#00-006-0230 International Centre for Diffraction Data, Newtown Square, PA (1996).
34. A. Pyne, K. Chatterjee, and R. Suryanarayanan. Crystalline to amorphous transition of disodium hydrogen phosphate during primary drying. *J. Pharm. Sci.* **20**:802–803 (2003).
35. A. Pyne, and R. Suryanarayanan. Phase transitions of glycine in frozen aqueous solutions and during freeze–drying. *Pharm. Res*. **18**:1448–1454 (2001). doi:10.1023/A:1012209007411.
36. I. Weissbuch, V. Y. Torbeev, L. Leiserowitz, and M. Lahav. Solvent effect on crystal polymorphism: why addition of methanol or ethanol to aqueous solutions induces the precipitation of the least stable β form of glycine. *Angew. Chem*. **44**:3226–3229 (2005). doi:10.1002/anie.200500164.
37. E. Y. Shalaev, D. V. Malakhov, A. N. Kanev, V. I. Kosyakov, F. V. Tuzikov, N. A. Varaksin, and V.I. Vavilin. Study of the phase diagram water fraction of the system water-glycine-sucrose by DTA and X-ray diffraction methods. *Thermochim. Acta.* **196**:213–220 (1992). doi:10.1016/0040-6031(92)85021-M.
38. T. Suzuki, and F. Franks. Solid-liquid phase transitions and amorphous states in ternary sucrose–glycine–water systems. *J. Chem. Soc. Farad. Trans*. **89**:3283–3288 (1993). doi:10.1039/ft9938903283.
39. R. Govindarajan, K. Chatterjee, L. Gatlin, R. Suryanarayanan, and E. Y. Shalaev. Impact of freeze–drying on ionization of sulfonephthalein probe molecules in trehalose-citrate systems. *J. Pharm. Sci*. **95**:1498–1510 (2006). doi:10.1002/jps.20620.
40. N. Blagden, R. J. Davey, M. Song, M. Quayle, S. Clark, D. Taylor, and A. Nield. A novel batch cooling crystallizer for *in situ* monitoring of solution crystallization using energy dispersive X-ray diffraction. *Cryst. Growth Des*. **3**:197–201 (2003). doi:10.1021/cg020053n.
41. C. Nunes. Use of high-intensity X-radiation in solid-state characterization of pharmaceuticals. Ph.D. dissertation, *Department of Pharmaceutics*, University of Minnesota, Minneapolis, 2005, p. 197.
42. C. Nunes, A. Mahendrasingam, and R. Suryanarayanan. Quantification of crystallinity in substantially amorphous materials by synchrotron X-ray powder diffractometry. *Pharm. Res*. **22**:1942–1953 (2005). doi:10.1007/s11095-005-7626-9.
43. A. P. Hammersley, M. Hanfland, A. N. Fitch, and D. Hausermann. Two-dimensional detector software: from real detector to idealized image or two-theta scan. *High Press. Res*. **14**:235–248 (1996). doi:10.1080/08957959608201408.
44. A. P. Hammersley. ESRF internal report, ESRF97HA02T. "Fit2D: an introduction and overview". (1997).